Zoomorphology (2022) 141:183–196
https://doi.org/10.1007/s00435-022-00554-8

ORIGINAL PAPER

Morphology of the feeding apparatus in two oxudercine gobies, *Parapocryptes serperaster* (Richardson 1846) and *Pseudapocryptes elongatus* (Cuvier 1816)

Loi X. Tran[1,2] · **Kiyoshi Soyano**[1,3] · **Atsushi Ishimatsu**[1,3,4]

Received: 2 July 2021 / Revised: 16 February 2022 / Accepted: 20 February 2022 / Published online: 8 March 2022

Abstract
Oxudercine gobies include fully aquatic to highly terrestrial species. In this study, we investigated the anatomy of the feeding apparatus of two species, *Parapocryptes serperaster* and *Pseudapocryptes elongatus*, both of which can be regarded as representing early stages of the transition from an aquatic to a terrestrial existence. The feeding system of these two species is morphologically similar: they both exhibit a unique orientation of premaxillary (vertical) and dentary (horizontal) teeth; a heterogeneous development of gill rakers among gill arches; strongly curved, large pharyngeal plates studded with numerous papilliform teeth; branchial basket skeletons with nearly equal gill-arch lengths; and a similar configuration of the branchial basket musculature. On the other hand, the number of teeth in *Pa. serperaster* is more than twice that in *Pd. elongatus*, both on the premaxillary and dentary bones, while the size of the teeth in *Pa. serperaster* is only half that in *Pd. elongatus* both in length and width. Pharyngeal plates and associated muscular and skeletal elements are more posteriorly positioned in *Pd. elongatus*. These similarities and differences may be explained by different trophic adaptations to herbivory and omnivory during the early transitional stages to life on mudflats. The results are discussed in the context of the two phylogenetic hypotheses of the oxudercine gobies based on their ecology and morphology and on genetic analysis.

Keywords Functional morphology · Feeding apparatus · Oxudercine gobies · *Parapocryptes serperaster* · *Pseudapocryptes elongatus*

Introduction

Oxudercine gobies offer a unique window through which we can glimpse how the form and function of the feeding system may be modified during transition from aquatic to terrestrial habitats (Clayton 2017; Tran et al. 2020, 2021). This group includes 43 species in ten genera (Murdy and Jaafar 2017), which live in a wide range of habitats, from shallow water to intertidal flats and supralittoral zones (Schöttle 1931; Clayton 1993, 2017; Ishimatsu and Ishimatsu 2021), exhibiting adaptations to herbivory, omnivory and carnivory (Clayton 1993, 2017).

In our previous paper (Tran et al. 2021), we compared the morphology of the feeding apparatus of five oxudercine species, *Boleophthalmus boddarti* (Pallas 1770), *Oxuderces nexipinnis* (Cantor 1849), *Scartelaos histophorus* (Valenciennes 1837), *Periophthalmus chrysospilos* Bleeker, 1853, and *Periophthalmodon schlosseri* (Pallas 1770). On the basis of the morphological analysis, the reported data on their feeding habits and degree of adaptation to terrestrial environments (terrestriality), and the widely accepted phylogenetic relationships of oxudercine genera (Murdy 1989; Murdy and Jaafar 2017), we hypothesized that the earliest oxudercine gobies that started to expand their niche onto land were herbivorous or omnivorous grazers, and that these gobies then diverged into more specialized herbivorous

✉ Loi X. Tran
txloi@ctu.edu.vn

1 Graduate School of Fisheries and Environmental Sciences, Nagasaki University, 1-14 Bunkyo-machi, Nagasaki 852-8521, Japan

2 College of Aquaculture and Fisheries, Can Tho University, 3/2 Street, Ninh Kieu District, Can Tho City, Vietnam

3 Institute for East China Sea Research, Organization for Marine Science and Technology, Nagasaki University, 1551-7 Taira-machi, Nagasaki 851-2213, Japan

4 Present Address: JICA CTU Project Office, Can Tho University, 3/2 Street, Ninh Kieu District, Can Tho City, Vietnam

species (*Boleophthalmus*) and carnivorous species (*Periophthalmus* and *Periophthalmodon*) through intermediate stages (*Scartelaos*) during the terrestrialization process. One a priori assumption was that the earliest fish that emerged from water had limited capacity to detect and capture food on land. Further, if the ecological factor that promoted land invasion was the presence of unexploited trophic resources on land ("the pull hypothesis", see Polgar 2017), then the food items of these fish are likely to have been ubiquitous and easily captured with little modification of their feeding mechanisms in water (Tran et al. 2021).

Parapocryptes serperaster (Richardson 1846) and *Pseudapocryptes elongatus* (Cuvier 1816) likely represent an early stage of transition from aquatic to amphibious life mode, even though relevant data are scarce: *Pa. serperaster* was reported to rarely move out of their burrows (Dinh et al. 2014). *Pd. elongatus* was observed to prefer shallow stagnant waters and seaward mudflats and tidal reaches of rivers or ponds (Takita et al. 1999), but the fish has also been photographed to feed on a mudflat surface (see Ishimatsu and Gonzales 2011). Thus, studying the anatomy of the feeding apparatus of these two species can be anticipated to shed light on how the feeding apparatus has been modified during the course of the niche expansion onto land by oxudercine gobies.

Materials and methods

Fish collection and preservation

Specimens of *Pa. serperaster* [172–192 mm in standard length (SL), $N = 37$] and *Pd. elongatus* (127–185 mm SL, $N = 33$) were collected at the Mo O mudflat (9° 26′ 15″ N, 106° 10′ 57″ E, Tran De District, Soc Trang Province, Vietnam) in December 2017 and June 2018 with bag nets. They were euthanized and preserved in a 10% neutralized formalin as reported by Tran et al. (2020, 2021). The total sample size of each species is larger than the sum of sample sizes given in the figures and tables because several different individuals were used to depict the structure of the feeding apparatus, for example, as given in Figs. 1, 3, 7, 9 and 11. This study was approved by the Animal Care and Use Committee of the Institute for East China Sea Research, Nagasaki University, Japan (Permit Number #16-01).

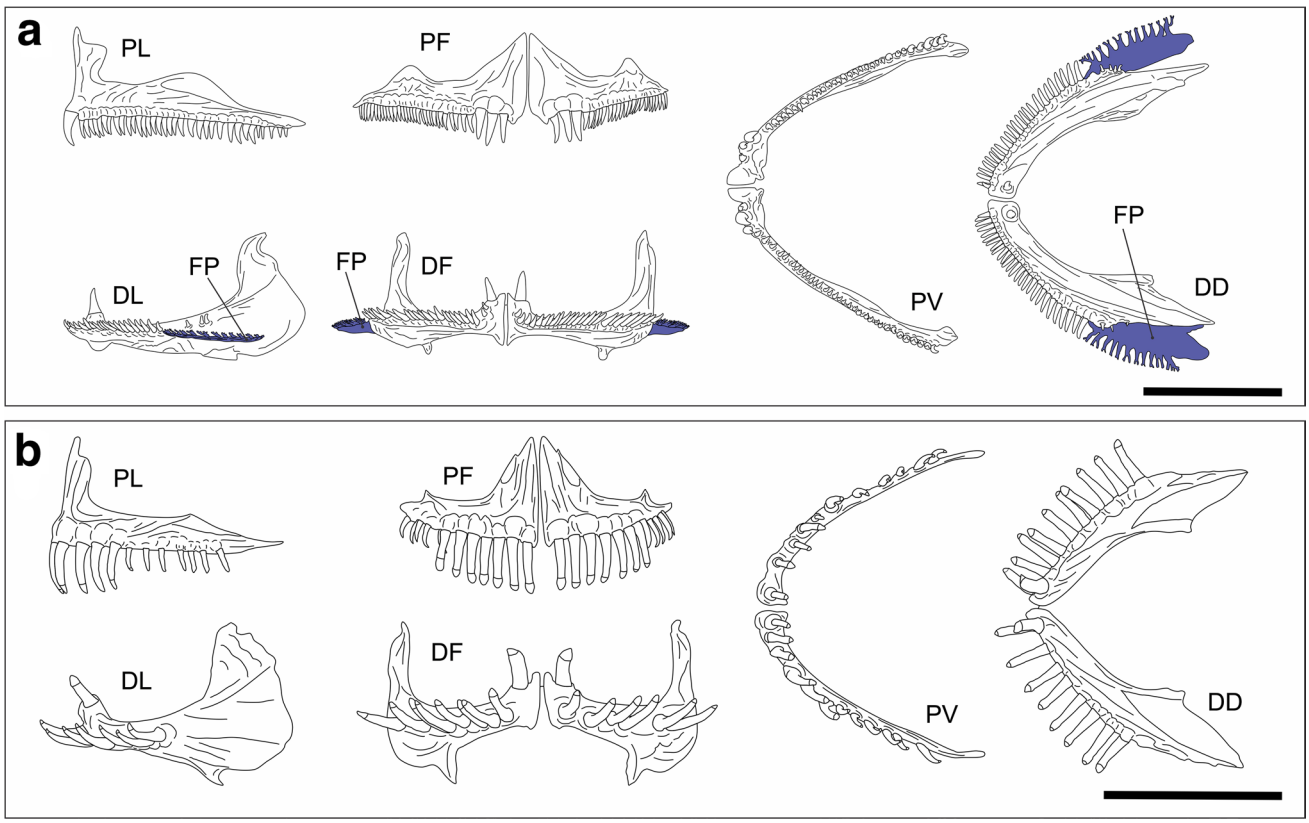

Fig. 1 Dentition of *Parapocryptes serperaster* (**a**) and *Pseudapocryptes elongatus* (**b**). *DD* dentary in dorsal view, *DF* dentary in frontal view, *DL* dentary in lateral view, *FP* finger-like projection, *PF* premaxilla in frontal view, *PL* premaxilla in lateral view, and *PV* premaxilla in ventral view. Scale bars: 5 mm

Morphological methods

Full account of the methods used in this study can be found in our previous papers (Tran et al. 2020, 2021). Briefly, we analyzed the morphology of four parts: oral jaws, gill rakers, pharyngeal plates, and branchial basket. The oral jaw was double-stained for cartilage and bones. The numbers of teeth and replacement teeth were counted, and the architecture of musculoskeletal system was analyzed, under a dissecting microscope. Tooth length and width were measured with ImageJ software (version 1.51J8, National Institutes of Health, USA), and the lever ratio of jaw closing (Westneat 2003) was calculated by dividing the length of the in-lever by the length of the out-lever, determined with ImageJ. The anatomy of the musculoskeletal system of the oral jaws was observed after clearing the samples. The number of gill rakers and the space between them were determined under the microscope, and the surface morphology of the gill rakers was observed with a scanning electron microscope (SEM, JSM-6380, JEOL, Tokyo, Japan) after the samples were dehydrated, dried and coated with palladium. The size of the pharyngeal plates was measured with ImageJ. The surface morphology and tooth density of the pharyngeal plates were observed and determined with the SEM. The branchial basket was dissected and double stained for the observation of musculoskeletal system and further cleared for the measurement of gill-arch lengths.

Statistical analysis

Tests of normality (Shapiro–Wilk test) and homogeneity of variance (Levene's test) were performed to analyze the measurements of dentition, gill rakers, gill-arch bones, pharyngeal plates, and tooth density of the pharyngeal plates. Based on these results, either the Student's *t* test with equal variance (data satisfied normal distribution and homogeneous variance), the Student's *t* test with unequal variance (data satisfied normal distribution but heterogeneous variance) or the Wilcoxon–Mann–Whitney test (data unsatisfied normal distribution) was performed to compare the number of teeth and replacement teeth, standardized tooth length, standardized tooth width, and relative size of the pharyngeal plates between the two species. One-way ANOVA followed by either post hoc Tukey tests (data satisfied normal distribution and equal variance) or post hoc Welch tests (data satisfied normal distribution but heterogeneous variance), or Kruskal–Wallis ANOVA followed by Wilcoxon–Mann–Whitney post hoc tests (data unsatisfied normal distribution) was performed to analyze the lengths of gill arches. Principal component analysis (PCA) based on a correlation matrix was performed to compare the dentition of seven species, two species of this study plus the five species investigated by Tran et al. (2021). All statistical analyses were performed in Rstudio version 0.99.903 (Rstudio, Inc). The packages "FactoMineR" (Lê et al. 2008) and "factoextra" (Kassambara and Mundt 2020) were used to perform the PCA, and the package "Rcmdr" (Fox 2005; Fox and Boutchet-Valat 2020) was used to perform the remaining analyses.

Results

Dentition

Both *Parapocryptes serperaster* and *Pseudapocryptes elongatus* have a single row of vertical teeth on the premaxilla. Frontal premaxillary teeth of *Pa. serperaster* and *Pd. elongatus* (3–4 pairs and 4–7 pairs, respectively) are larger and fang like; those of *Pd. elongatus* also have enlarged cusps, and all premaxillary teeth are sparser in this species (Fig. 1a, b). Both species have a single row of dentary teeth that extend horizontally and a pair of fang-like symphyseal teeth (Fig. 1a, b). *Pa. serperaster* possesses a cartilaginous finger-like projection extending laterally along the posterior margin of the dentary (Fig. 1a). Teeth in *Pa. serperaster* are significantly more numerous and smaller than in *Pd. elongatus*, while the number of replacement teeth is not significantly different between the two species (Table 1).

Figure 2 shows a PCA biplot of the eight variables related to dentition given in Table 1 together with the data for the five oxudercine species (*B. boddarti*, *O. nexipinnis*, *Pn. schlosseri*, *Ps. chrysospilos*, and *S. histophorus*) reported by Tran et al. (2021). The seven species are separated into three groups in the multivariate space (Fig. 2). The first two components (PC1 and PC2) explain 77.8% of total variance. Along the PC1 axis, *Pa. serperaster* and *B. boddarti* are separated from the other species by their higher number of teeth, and smaller values of the standardized tooth length and tooth width on both the premaxilla and dentary. Along the PC2 axis, *Pa. serperaster* is associated with *B. boddarti*, while *Pd. elongatus* is associated with *O. nexipinnis* and *S. histophorus*. *Ps. chrysospilos* and *Pn. schlosseri* are separated from the other species by their lower number of teeth and higher number of replacement teeth both on the premaxilla and dentary.

Oral jaw bones and muscles

The lever ratio of jaw closing is 0.42 ± 0.01 (mean $\pm$ SD, $N = 3$) in *Pa. serperaster* and 0.47 ± 0.02 in *Pd. elongatus*. Both species have the maxillo-mandibular ligament (L1) and the premaxillo-maxillary ligament (L2, Fig. 3). In both species, the adductor mandibulae A1, A2, and A3 attach onto the maxilla, the coronoid process of the dentary, and the medial side of the dentary, respectively.

Table 1 Dentition of *Parapocryptes serperaster* and *Pseudapocryptes elongatus*

Species	Premaxilla				Dentary			
	Number of teeth	Number of replacement teeth	Standardized tooth length ($\times 10^{-3}$)	Standardized tooth width ($\times 10^{-3}$)	Number of teeth	Number of replacement teeth	Standardized tooth length ($\times 10^{-3}$)	Standardized tooth width ($\times 10^{-3}$)
Parapocryptes serperaster	67.6 ± 2.3	8.6 ± 2.3	3.2 ± 0.7	0.9 ± 0.1	53.0 ± 2.7	6.8 ± 2.3	3.2 ± 0.8	0.9 ± 0.1
Pseudapocryptes elongatus	30.3 ± 3.1	7.0 ± 2.0	6.4 ± 1.0	1.8 ± 0.3	20.2 ± 2.9	5.2 ± 0.8	7.1 ± 1.1	1.9 ± 0.4
Student's *t*-test or Wilcoxon test								
T or *W* values	66$^{\#\#}$	− 1.24$^{\#}$	5.59$^{\#}$	6.45$^{\#}$	0.78$^{\#\#}$	7.5$^{\#\#}$	6.48$^{\#}$	25$^{\#\#}$
p	0.004	0.25	< 0.001	< 0.001	0.005	0.19	< 0.001	0.008

The number of teeth represents the sum of teeth on both sides. The other data are for the values on left side only (mean ± SD, $N = 5$). Student's *t*-test$^{\#}$ or Wilcoxon test$^{\#\#}$ was applied for comparison. Tooth length and tooth width do not include fang-like symphyseal teeth and were standardized by the standard length. Tooth width was measured at the tooth's point of insertion into the premaxillary or dentary bone

Gill rakers

The branchial basket of *Pa. serperaster* and *Pd. elongatus* comprises four pairs of gill arches with two rows of gill rakers along each arch. The morphology of the gill rakers of the two species is similar with short and sparsely spaced gill rakers on the first, second and anterior row of the third arch, and comb-like and more densely spaced gill rakers on the posterior row of the third arch and both rows of the fourth arch (Figs. 4, 5, and 6). There are significant differences in the number and the space between gill rakers of respective rows of the two species, except the number of gill rakers on the posterior row of the second arch (Figs. 5 and 6). The gill rakers extend laterally from the inner surface (facing the oropharyngeal cavity) of gill arches along their entire lengths. Each gill raker blade has a triangular shape in cross section both in *Pa. serperaster* (Fig. 4a1 and a2) and *Pd. elongatus* (Fig. 4b1 and b2).

Pharyngeal plates

The pharyngeal plates of the two species are similar in having a strong curvature of the plates (Fig. 7a and b), numerous fine papilliform teeth and less numerous canine teeth (along the anterior and medial margins of both plates) both in dorsal and ventral pharyngeal plates (Fig. 8a and b, Table 2), and the overlapping of the third and fourth pharyngobranchials (PB3 and PB4) to form one large unit of the dorsal pharyngeal plate (Fig. 9a and b). The papilliform teeth on the ventral pharyngeal plates of both species are arranged in lines and are hook like (Fig. 8a4, a5, b4, and b5). Interspecific differences include the size of the plates (Fig. 10), the density of papilliform teeth on the dorsal plate (Table 2) and the orientation of both types of teeth (Fig. 8a1 and a2 for *Pa. serperaster*; Fig. 8b3 and b6 for *Pd. elongatus*; see also Table 2), and a larger overlap between PB3 and PB4 in *Pa. serperaster* (Fig. 9a1) than in *Pd. elongatus* (Fig. 9b1).

Branchial basket skeleton

The ratios of length to width of the first to fourth ceratobranchials (CB1-4, mean ± SD, $N = 3$) are 14.96 ± 3.80 in *Pa. serperaster* and 13.48 ± 1.99 in *Pd. elongatus*. The basihyal (BH) is bifurcated in *Pa. serperaster* (Fig. 9a), but flabelliform in *Pd. elongatus* (Fig. 9b). The second pharyngobranchial (PB2) extends along the anterior margin of the PB3 and PB4 in both species (Fig. 9a1, b1). The fourth epibranchial (EB4) is L-shaped (91.2 ± 0.8°, mean ± SD, $N = 5$) and more flattened medially in *Pa. serperaster* (Fig. 9a2), but more obtuse (117.7 ± 1.2°, $N = 6$) and relatively slender in *Pd. elongatus* (Fig. 9b2). There is no significant difference among the gill-arch lengths between the two species (Table 3).

Branchial basket musculature

The branchial basket musculature of the two species consists of four systems. The first system connects the element bones of the branchial basket to the surrounding skeletal components: the levatores interni (LI, LI'), the levatores externi (LE1-4), the levator posterior (LP), the retractor dorsalis (RD), the pharyngohyoideus (PH), the rectus ventralis (RV3), the pharyngocleithralis externus (PHCE), and the pharyngocleithralis internus (PHCI) (Fig. 11a3 and b3). The second system connects element bones dorsally: the paired transversi dorsales anteriores (TDA), the paired transversi dorsales posteriores (TDP), and the obliqui dorsales (OD), all connected to a medial structure resembling the cartilaginous cushion (CC) described by

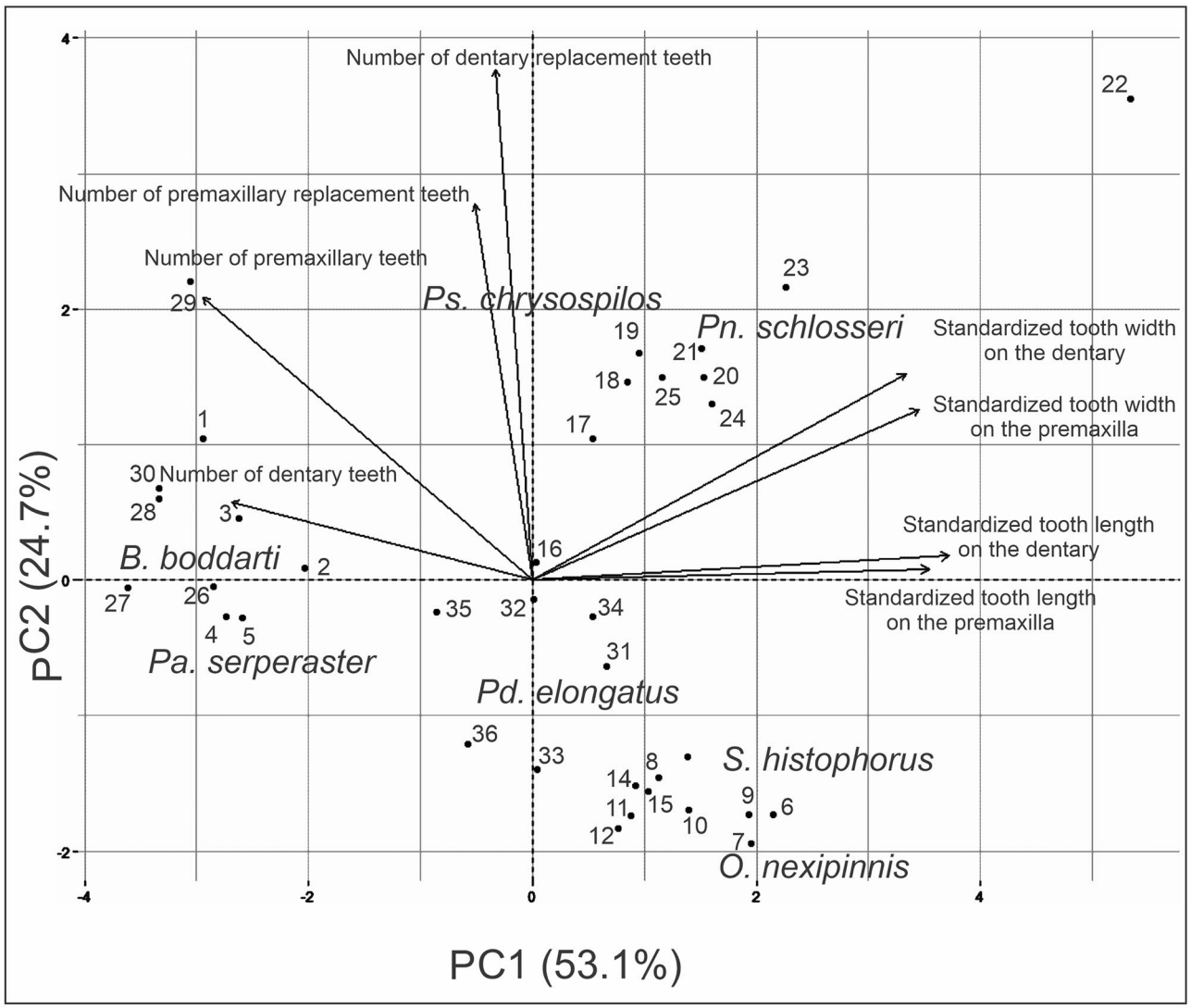

	PC1	PC2
Number of premaxillary teeth	-0.75	0.53
Number of premaxillary replacement teeth	-0.13	0.71
Standardized length of premaxillary teeth	0.90	0.02
Standardized width of premaxillary teeth	0.88	0.32
Number of dentary teeth	-0.68	0.15
Number of dentary replacement teeth	-0.08	0.96
Standardized length of dentary teeth	0.95	0.04
Standardized width of dentary teeth	0.85	0.39

Fig. 2 PCA biplot of the two principal components (PC1, PC2) showing the multivariate ordination of *Parapocryptes serperaster, Pseudapocryptes elongatus* and the five mudskipper species studied by Tran et al. (2021, upper box). The morphological variables are represented by vectors; correlated variables have a similar orientation. Loadings of each variable along PC1 and PC2 are shown in the lower table. Points 1–5 are for *Boleophthalmus boddarti*, 6–10 *Oxuderces nexipinnis*, 11–15 *Scartelaos histophorus*, 16–20 *Periophthalmus chrysospilos*, 21–25 *Periophthalmodon schlosseri*, 26–30 *Parapocryptes serperaster*, and 31–36 *Pseudapocryptes elongatus*

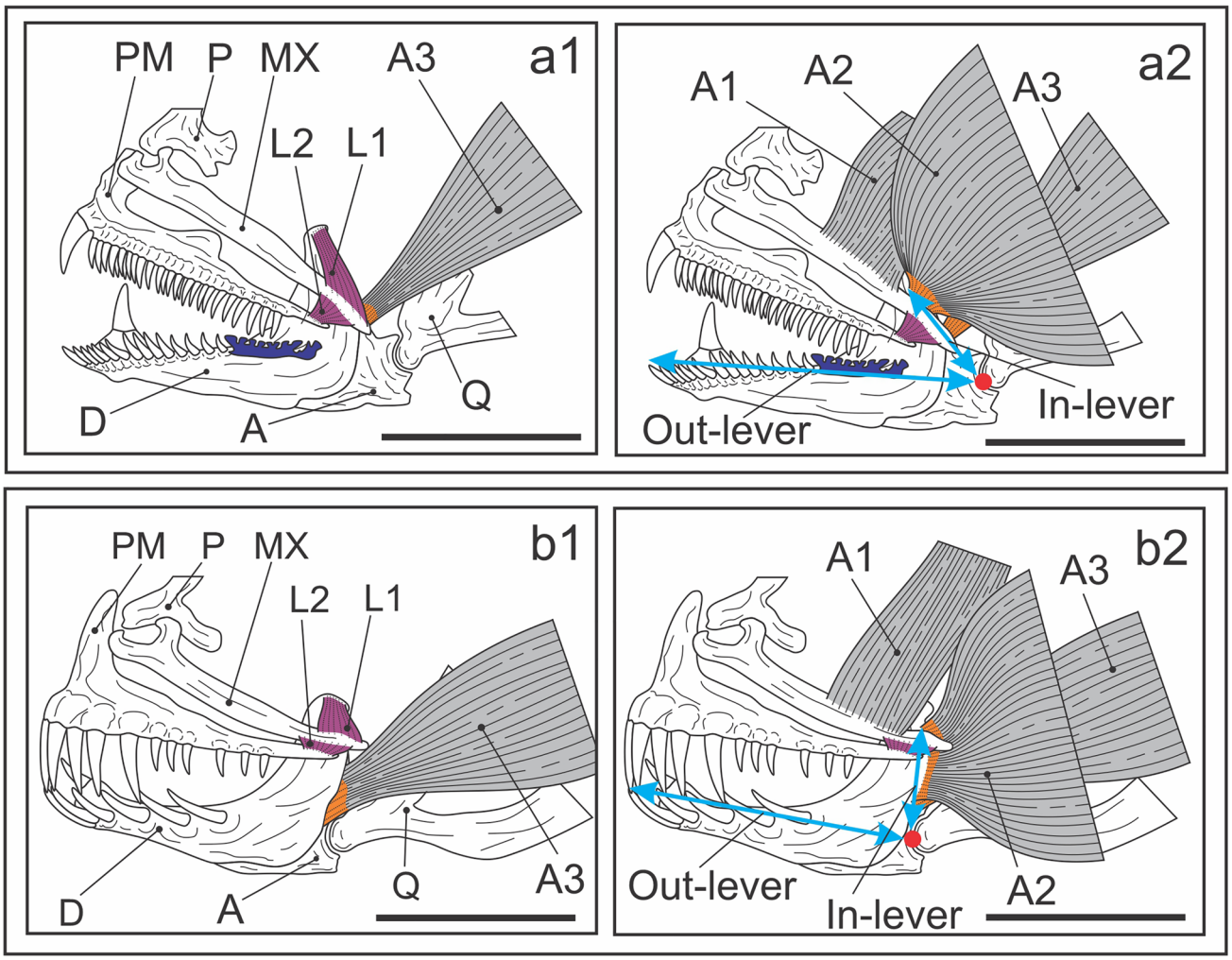

Fig. 3 Jaw bones, ligaments and adductor mandibulae in *Parapocryptes serperaster* (**a1** and **a2**) and *Pseudapocryptes elongatus* (**b1** and **b2**). *A* articular, *A1–3* adductor mandibulae 1–3, *D* dentary, *L1*, *2* ligaments 1 (maxillo-mandibular) and 2 (premaxillo-maxillary), *MX* maxilla, *P* palatine, *PM* premaxilla, *Q* quadrate. Ligaments are shown in purple and tendons are in orange. In **a2** and **b2**, the red dot shows the fulcrum, and the double-headed arrows (blue) show the jaw-closing lever system. Scale bars: 5 mm

Liem (1974), and a ligament (L3-4) connecting the third and fourth epibranchials (Fig. 11a1 and b1). The third system connects the element bones ventrally: the transversi ventrales (TV1-5), the obliqui ventrales (OV1-4), and the semicircular ligament (SL) (Fig. 11a2 and b2). The fourth system connects the ceratobranchials to the epibranchials (Fig. 11a3 and b3). RD connects to the anterior portion of the fourth vertebra in both species (Fig. S1). When viewed dorsally, the muscles of the second system are positioned more posteriorly in *Pd. elongatus* (Fig. 11b1) than in *Pa. serperaster* (Fig. 11a1).

Discussion

Comparison of the feeding apparatus of *Pa. serperaster* and *Pd. elongatus*

The feeding apparatus of *Parapocryptes serperaster* and *Pseudapocryptes elongatus* shares similar morphologies in several respects, but there are also differences. Similarities include the orientation of premaxillary (vertical) and

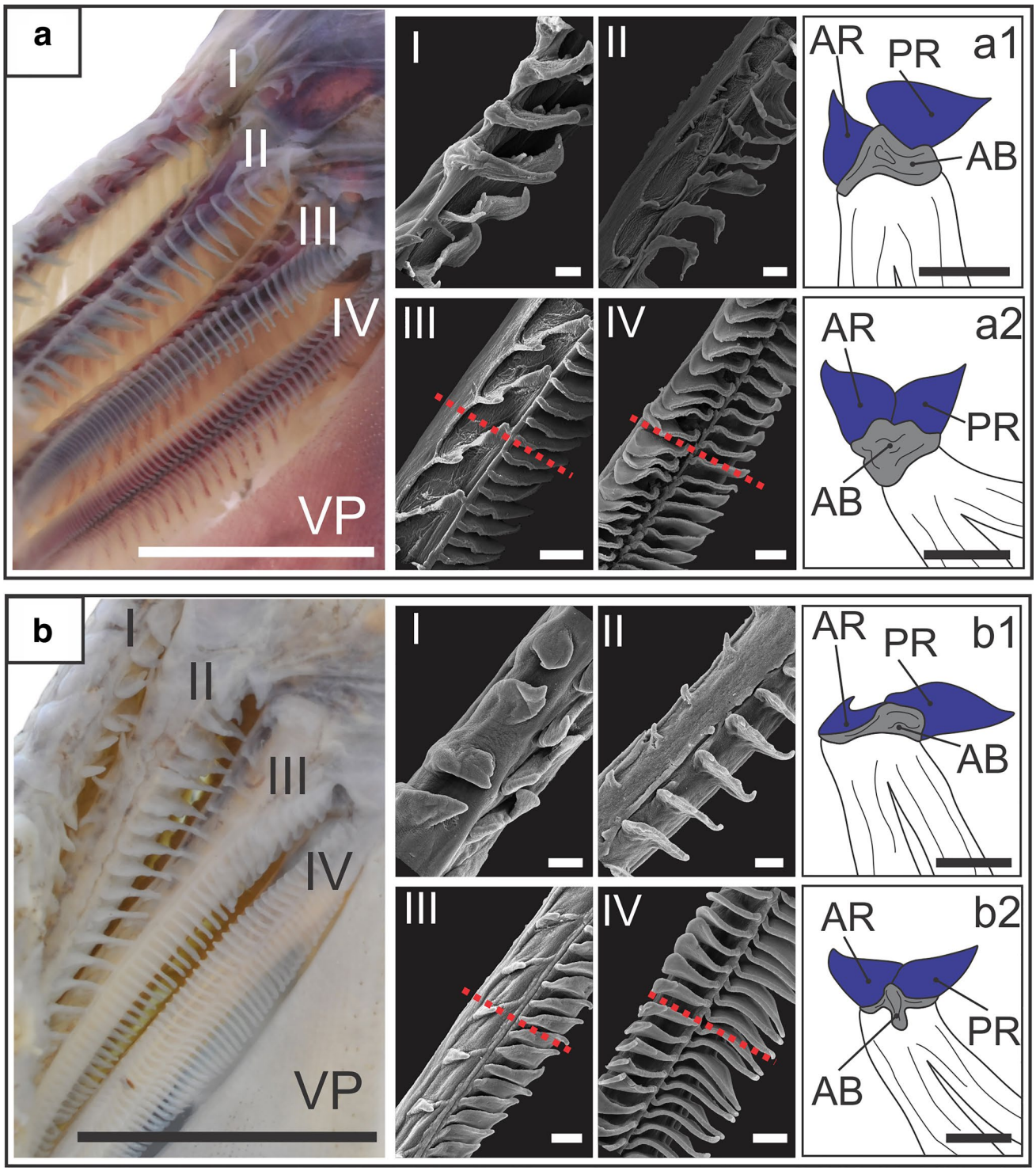

Fig. 4 Morphology of the gill rakers in *Parapocryptes serperaster* (**a**) and *Pseudapocryptes elongatus* (**b**). In each box, the left photograph shows the dorsal view of the left gill arches, and the right ones are SEM micrographs of each gill arch. The red dashed lines in the SEM micrographs indicate the position of cross sectioning. Cross-sectional views of the third and fourth arches are shown in **a1**, **a2**, **b1**, and **b2**. *AB* arch bone, *AR* anterior row, *I–IV* first to fourth gill arches, *PR* posterior row, *VP* ventral pharyngeal plate. Scale bars: 2 mm for the photographs, 200 µm for SEM micrographs, and 0.5 mm for **a1**, **a2**, **b1**, and **b2**

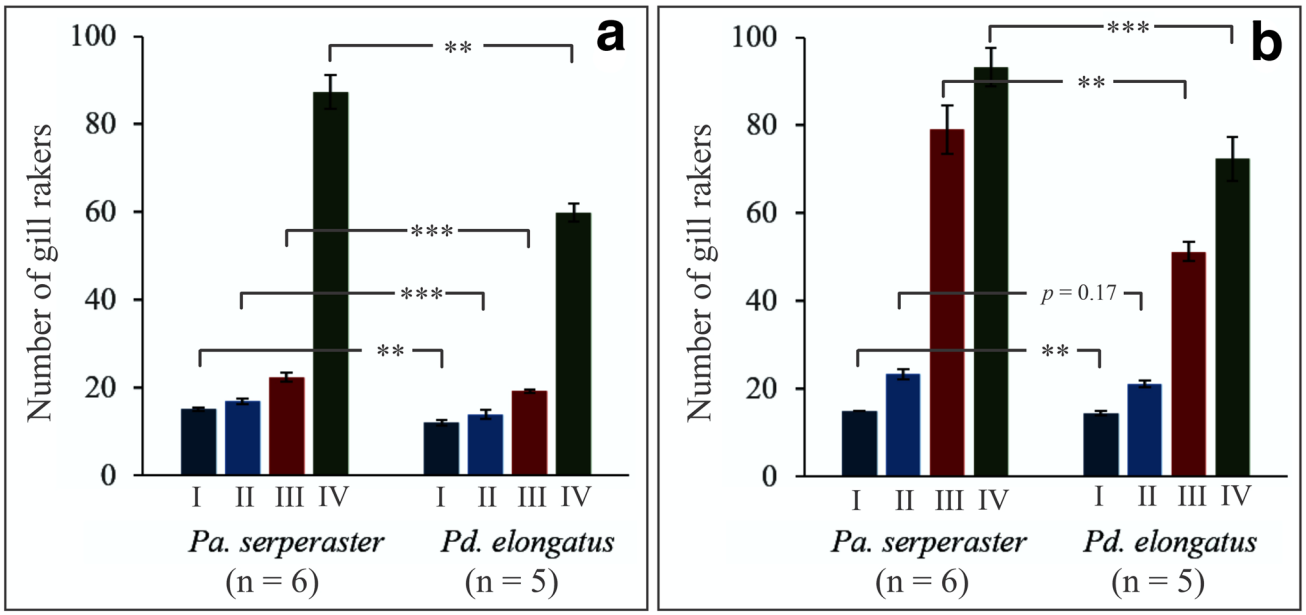

Fig. 5 Number of gill rakers (mean ± SD) on the anterior (**a**) and posterior (**b**) gill arches of *Parapocryptes serperaster* and *Pseudapocryptes elongatus*. *I–IV* first to fourth gill arches. Size range of *Parapocryptes serperaster*: 154–186 mm in standard length (SL) and *Pseudapocryptes elongatus*: 150–167 mm SL. The number of individuals used for the analysis is given in the parentheses. Student's *t* test or Wilcoxon test was applied for comparison of the parameters. Statistical significance was declared at the 5% level. Asterisks (** < 0.001, *** < 0.0001) show significant differences of respective rows of gill rakers between the two species

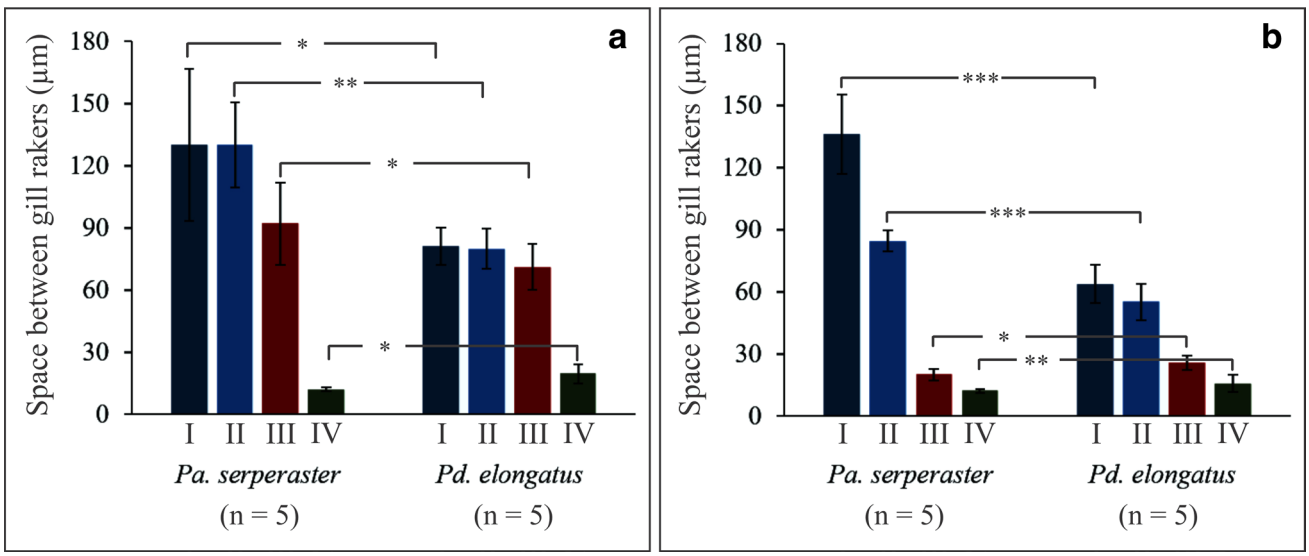

Fig. 6 Average space between the gill rakers (mean ± SD) on the anterior (**a**) and posterior (**b**) gill arches of *Parapocryptes serperaster* and *Pseudapocryptes elongatus*. Symbols and fish size ranges as in Fig. 5. Number of individuals used for the analysis is given in the parentheses. Student's *t* test or Wilcoxon test was applied for comparison of the parameters. Statistical significance was declared at the 5% level. Asterisks (* < 0.05, ** < 0.001, *** < 0.0001) show significant differences of respective rows of gill rakers between the two species

dentary (horizontal) teeth, the heterogeneous development of gill rakers among gill arches, the strongly curved pharyngeal plates studded with numerous papilliform teeth as well as fewer canine teeth, branchial basket skeletons with nearly equal standardized gill-arch lengths, and a similar configuration of the branchial basket musculature. On the other hand, the most notable interspecific difference is the number and size of oral teeth. Both premaxillary

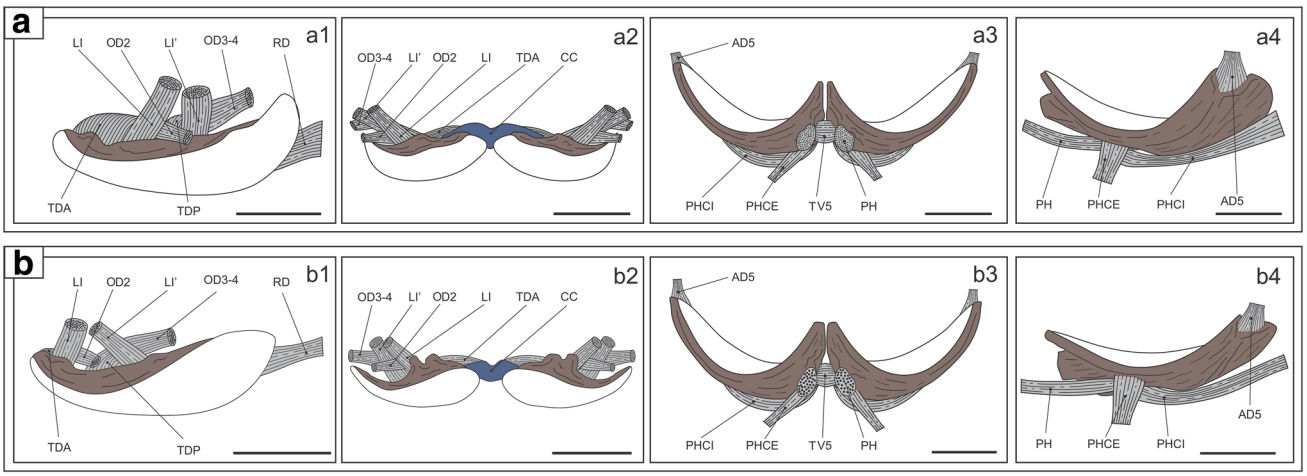

Fig. 7 Morphology of the pharyngeal plates and the muscular system attaching to them in *Parapocryptes serperaster* (**a**) and *Pseudapocryptes elongatus* (**b**). **a1**, **b1** Lateral views of the left dorsal pharyngeal plates; **a2**, **b2** frontal views of the dorsal pharyngeal plates; **a3**, **b3** frontal views of the ventral pharyngeal plates; **a4**, **b4** lateral views of the left ventral pharyngeal plates. *AD5* adductor 5, *CC* cartilaginous cushion, *LI* and *LI'* levatores interni, *OD2–4* obliqui dorsales 2 to 4, *PH* pharyngohyoideus, *PHCE* pharyngocleithralis externus, *PHCI* pharyngocleithralis internus, *RD* retractor dorsalis, *TDA* transversus dorsalis anterior, *TDP* transversus dorsalis posterior, *TV5* tranversi ventrales 5. The dorsal side of the dorsal pharyngeal plates and the ventral side of the ventral pharyngeal plates are colored in brown. Scale bars: 2 mm

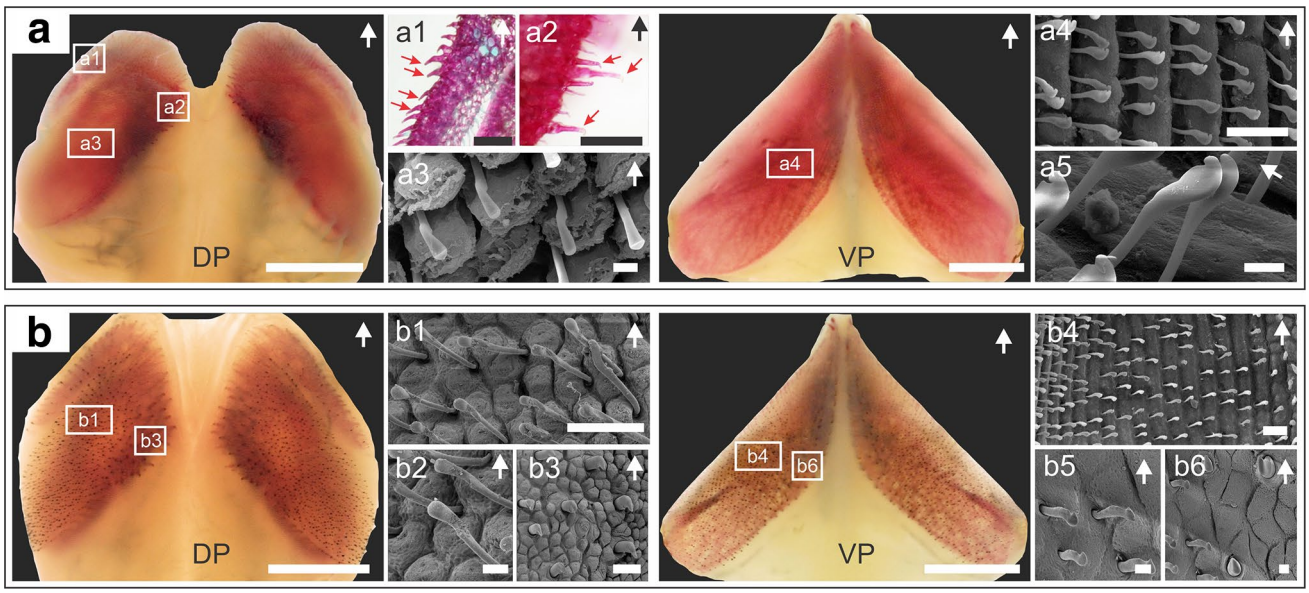

Fig. 8 Morphology of the pharyngeal plates of *Parapocryptes serperaster* (**a**) and *Pseudapocryptes elongatus* (**b**). Larger color photographs show surface views of the dorsal (DP) and ventral (VP) pharyngeal plates. Light microscopy (**a1**, **a2**) and SEM micrographs (**a3**, **a4**, **b1**, **b3**, **b4**, **b6**) correspond to the named white boxes in the larger color photographs. **a5**, **b2**, and **b5** show pharyngeal teeth at higher magnifications of **a4**, **b1**, and **b4**, respectively. Red arrows in **a1** and **a2** show canine teeth on the marginal edge of the right dorsal pharyngeal plate. Arrows on the upper right corners of color photographs and the SEM micrographs indicate the anterior orientation. Scale bars: 2 mm for color photographs; 500 µm for **a1-2**; 100 µm for **a4**, **b1**, **b3**, **b4**, and 20 µm for **a3**, **a5**, **b2**, **b5,** and **b6**

and dentary teeth in *Pa. serperaster* are more than twice as many, but only half the size both in length and width as compared with *Pd. elongatus*. In addition, the relative size of the pharyngeal plates and the density of papilliform teeth of the dorsal plates are larger in *Pa. serperaster* than in *Pd. elongatus*. The density of papilliform teeth of the ventral plates is also larger in *Pa. serperaster* than in *Pd.*

Table 2 Tooth morphology, density, and direction of the pharyngeal plates of *Parapocryptes serperaster* and *Pseudapocryptes elongatus*

Species	Shape	Density (number/mm^2)		Direction	
		Dorsal plate	Ventral plate	Dorsal plate	Ventral plate
Parapocryptes serperaster	Papilliform	515.4 ± 83.4	209.5 ± 33.3	PM	PM
	Canine*			DV	DV
Pseudapocryptes elongatus	Papilliform	187.3 ± 35.4	149.0 ± 14.3	DV	PM
	Canine*			Posterior	Anterior
Student's *t*-test (*t*-value)		− 6.39	− 2.95		
p		0.012	0.073		

DV dorsoventral, *PM* posteromedial

*Along the anterior and medial margins of the dorsal and ventral plates. Mean ± SD, $N = 3$ for *Pa. serperaster*, $N = 4$ for *Pd. elongatus*. Student's *t*-test was applied for comparison of tooth density between the two species

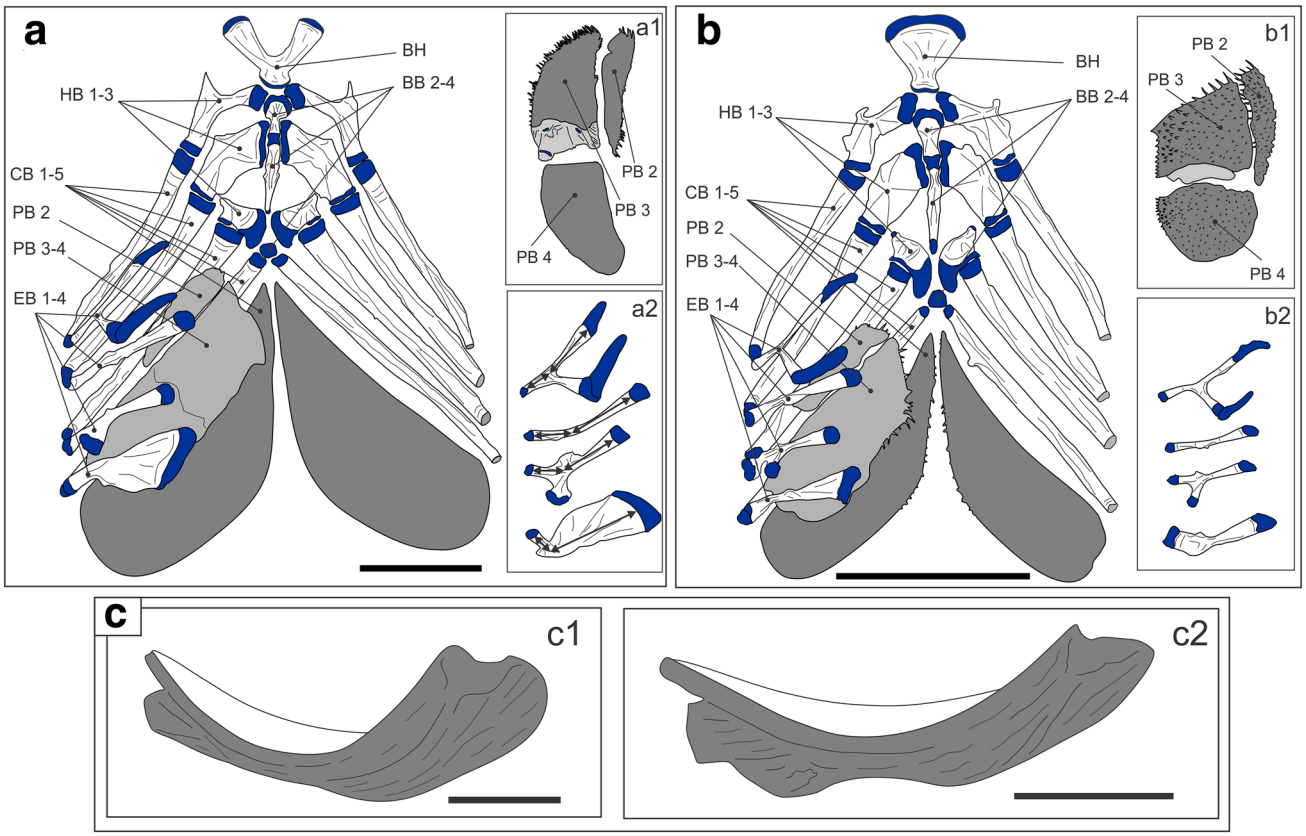

Fig. 9 Morphology of the branchial basket skeleton (dorsal view) and the left fifth ceratobranchial (= ventral pharyngeal plate, lateral view) of *Parapocryptes serperaster* (**a**, **c1**) and *Pseudapocryptes elongatus* (**b**, **c2**). BB 2–4 basibranchials 2–4, BH basihyal, CB 1–5 ceratobranchials 1–5, EB 1–4 epibranchials 1–4, HB 1–3 hypobranchials 1–3, PB 2–4 pharyngobranchials 2–4. BB1 is a small cartilage between the right and left HB1s (not shown). **a1**, **b1**: left dorsal pharyngeal plate in ventral view; **a2**, **b2**: right epibranchials in ventral view. The portion of PB3 covered by PB4 is shown in light gray in **a1** and **b1**. Cartilages are in blue. The ventral surface of the fifth ceratobranchial is in dark gray in **c**. Double-headed arrows in **a2** indicate length measurements. Scale bars: 5 mm for boxes **a** and **b**, 2 mm for box **c**

elongatus, but the difference is only marginal ($p = 0.073$), probably due to the small sample size (Table 2).

The morphological similarities of the feeding apparatus probably reflect adaptations to feeding on minute food items (microalgae and detritus) in environments with a high concentration of mud particles. The morphological differences may be related to an incipient shift to omnivory and possibly also to terrestrial feeding in *Pd. Elongatus*, but not in *Pa.*

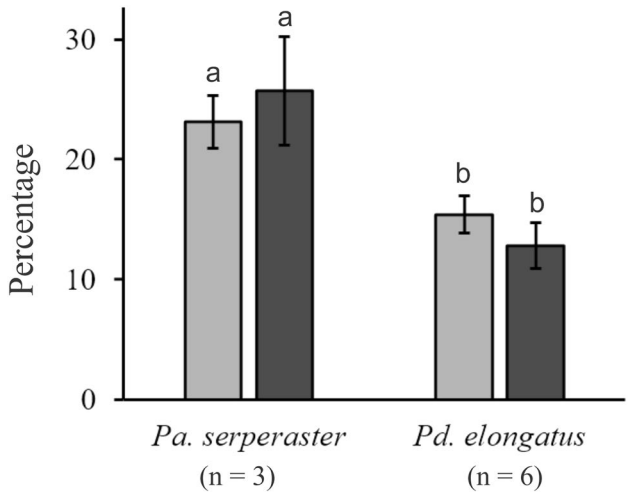

Fig. 10 The relative size (area of pharyngeal plates/frontal sectional area of the dorsal or ventral surface of the oropharyngeal cavity) (mean ± SD) of the dorsal (light gray bars) and ventral (dark gray bars) pharyngeal plates. Student's *t* test and Wilcoxon test were performed to compare the relative size of the dorsal and ventral pharyngeal plates between the two species, respectively. Data with different letters of the dorsal or ventral pharyngeal plate are significantly different ($p < 0.05$). The number of individuals used for the measurement is given in parenthesis

serperaster. *Pa. serperaster* was reported to feed mainly on diatoms and detritus (Dinh et al. 2017) or exclusively on diatoms (Khaironizam and Norma-Rashid 2000). In comparison, *Pd. elongatus* in the Mekong Delta (Bucholtz et al. 2009) and in the Gulf of Thailand (Swennen et al. 1995) was reported to feed on diatoms, but the fish in the Indian Sundarbans was found to be omnivorous (food items consisting of phytoplankton, small crustaceans, aquatic insects and fish, Chaudhuri et al. 2014). In addition, *Pa. serperaster* seem to feed exclusively in water when their habitat is covered by water during high tide, because the fish were rarely observed out of their burrows (Dinh et al. 2014). In contrast, *Pd. elongatus* feed not only in water, but at least for some populations also on land. We observed that the fish in the Mekong Delta fed mostly in shallow water (see supplementary video S1), but there is also evidence of the fish feeding on an exposed mudflat in Penang, Malaysia (see Fig. 4.5.5 of Ishimatsu and Gonzales 2011, a photograph taken by the late Professor Toru Takita).

Comparison with the feeding apparatus of other mudskippers

The morphology of the feeding apparatus in *Pa. serperaster* and *Pd. elongatus* is qualitatively and quantitatively similar to that of *Boleophthalmus* mudskippers, which graze epipelic diatoms and other microalgae on exposed mudflat surfaces during low tide (*B. boddarti*, Swennen et al. 1995; Chaudhuri et al. 2014; Tran et al. 2021, *B. dussumieri*, Rathod and Patil 2009; and *B. pectinirostris*, Yang et al. 2003, Tran et al. 2020). The orientation of the premaxillary and that of the dentary teeth, the morphology of pharyngeal plates, and the unique disposition of gill rakers are all shared features between *Pa. serperaster*, *Pd. elongatus* and *Boleophthalmus* species.

Of the two species studied here, *Pa. serperaster* is more similar to *Boleophthalmus* mudskippers in the morphology of feeding apparatus than *Pd. elongatus*. The bifurcated basihyal and the L-shaped EB4 are common only between *Pa. serperaster*, *B. boddarti* and *B. pectinirostris*, but not seen in *Pd. elongatus*. The seemingly stronger reliance on microalgal grazing in *Pa. serperaster* than in *Pd. elongatus* is probably reflected in the occurrence of more numerous, finer oral teeth in *Pa. serperaster*. In fact, the number of premaxillary teeth in *Pa. serperaster* is nearly identical with the number reported for *B. boddarti* (65.6 ± 5.1, Tran et al. 2021) and *B. pectinirostris* (66.4 ± 5.8, Tran et al. 2020), and the number of the dentary teeth in *Pa. serperaster* is about 70% of the values reported for *B. boddarti* (78.8 ± 2.8) and *B. pectinirostris* (74.6 ± 3.2). The unique morphology of the dentary teeth seen in *Boleophthalmus* species, i.e., anteriorly directed flexure and occasional overlapping at the most distal part is absent in *Pa. serperaster*. The specialized dentary teeth morphology, higher density of gill rakers on the three most posterior rows, and more numerous papilliform teeth in the pharyngeal plates in *Boleophthalmus* mudskippers than in *Pa. serperaster* (except papilliform-teeth density in the dorsal pharyngeal plate of *B. pectinirostris*) might attest to an increasing need for efficient food–mud separation

Table 3 Comparison of the gill-arch lengths (mean ± SD) of *Parapocryptes serperaster* and *Pseudapocryptes elongatus*

	Arch length (mm)						
	N	Arch 1	Arch 2	Arch 3	Arch 4	ANOVA	
						F	*p*
Parapocryptes serperaster	6	18.9 ± 2.3	19.8 ± 2.1	19.0 ± .1	20.8 ± 2.0	1.0	0.40
Pseudapocryptes elongatus	7	13.9 ± 1.8	12.9 ± 1.6	12.3 ± 1.6	12.6 ± 1.7	1.1	0.36

No significant difference was detected for the arch length in each species (one-way ANOVA)

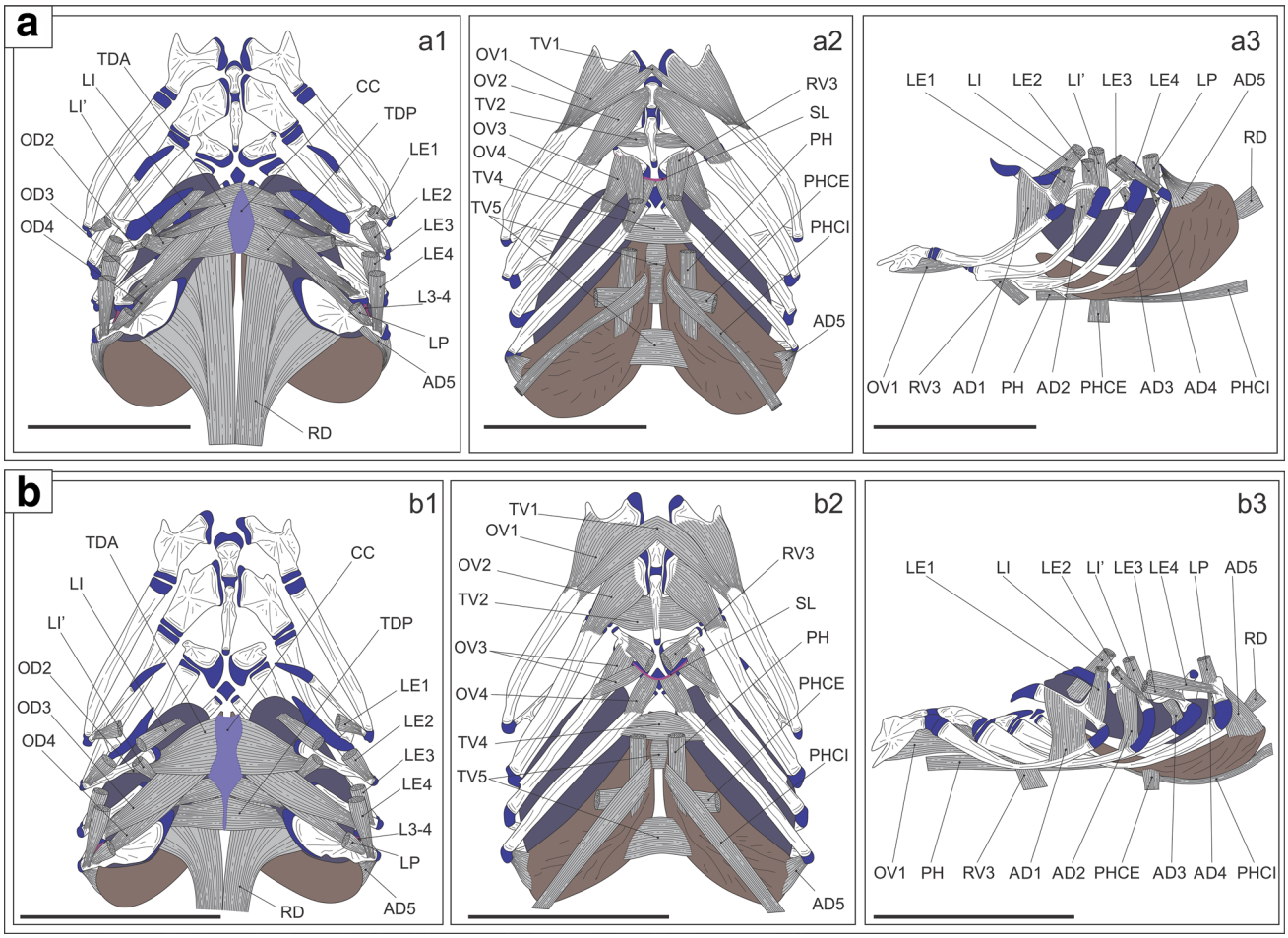

Fig. 11 Morphology of the branchial basket musculature of *Parapocryptes serperaster* (**a**) and *Pseudapocryptes elongatus* (**b**). **a1** and **b1** are dorsal views, **a2** and **b2** ventral views, while **a3** and **b3** are lateral views. *AD1–5* adductors 1 to 5, *CC* cartilaginous cushion, *L3–4* ligaments 3–4 connecting the third and fourth epibranchials, *LE1–4* levatores externi 1–4, *LI* and *LI'* levatores interni, *LP* levator posterior, *OD2–4* obliqui dorsales 2–4, *OV1–4* obliqui ventrales 1–4, *PH* pharyngohyoideus, *PHCE* pharyngocleithralis externus, *PHCI* pharyngocleithralis internus, *RD* retractor dorsalis, *RV3* rectus ventralis 3, *SL* semicircular ligament, *TDA* transversus dorsalis anterior, *TDP* transversus dorsalis posterior, *TV1–5* tranversi ventrales 1–5. Note that *TV3* is absent in these species. Cartilages in blue; dorsal pharyngeal plate in dark purple; ventral pharyngeal plate in brown. Scale bars: 5 mm

during terrestrial feeding than the aquatic feeding by *Pa. serperaster*.

Pd. elongatus, *O. nexipinnis* and *S. histophorus* have much fewer and longer oral teeth than *Pa. serperaster* and *Boleophthalmus* mudskippers (Fig. 1, see also Tran et al. 2021), which may be related to their tendency toward omnivory. It should be noted, however, their feeding habits seem to vary between populations of the same species as well as between species of the same genus. *O. nexipinnis* (reported as *O. dentatus*) in Sundarbans was reported to be omnivorous, feeding on phytoplankton, zooplankton, aquatic insects and detritus by Chaudhuri et al. (2014) but we found that *O. nexipinnis* in the Mo O mudflat exclusively fed on diatoms (Tran et al. 2021). *S. histophorus* was reported to be omnivorous, feeding mainly on diatoms and polychaetes for the population in Hong Kong by Chan (1989) or on diatoms and amphipods for the population in Mo O by Tran et al. (2021), but a congener *S. tenuis* in the Persian Gulf was reported to feed on mussels, shrimps and crabs by Abidizadegan et al. (2015). Comparison of the feeding apparatus between different populations of *O. nexipinnis* as well as between *S. histophorus* and *S. tenuis* might provide further insights into how feeding habits could affect the morphology of feeding apparatus in oxudercine gobies.

The feeding ecology and phylogeny of mudskippers

In our previous paper (Tran et al. 2021), we hypothesized that the early oxudercine gobies that started to expand their niche onto land were herbivorous or omnivorous grazers. The hypothesis was based on the phylogenetic relationships of the oxudercine gobies based on the ecological and

morphological characteristics by Murdy (1989), the feeding habits and the terrestriality among the ten oxudercine genera. In Murdy's diagram, the subfamily Oxudercinae is monophyletic, and divided into a clade consisting of *Apocryptodon*, *Oxuderces* and *Parapocryptes* and the other clade comprising the other genera. The three genera (*Boleophthalmus*, *Periophthalmodon* and *Periophthalmus*) are the most derived within the subfamily Oxudercinae and equipped with the highest capacity for terrestrial activities. When the feeding habits are overlaid in this diagram, the genera with no (*Apocryptodon*) or low (*Apocryptes*, *Oxuderces*, *Parapocryptes* and *Pseudapocryptes*) degrees of terrestriality are mostly herbivorous or omnivorous, and the three most terrestrial genera are either highly specialized herbivores (*Boleophthalmus*) or purely carnivores (*Periophthalmodon* and *Periophthalmus*, see Table S1 of Tran et al. 2021 on the feeding habit of the oxudercine gobies). The feeding habit of *Zappa* (only one species, *Z. confluentus*, is known) is currently unknown. Thus, we speculate that during the terrestrialization process, oxudercine gobies might have diverged into specialized herbivorous species (*Boleophthalmus*) and carnivorous species (*Periophthalmus* and *Periophthalmodon*) through intermediate stages as seen in *Scartelaos*.

In contrast, the molecular phylogeny proposed by Steppan et al. (2022) indicated a clade consisting of oxudercine (the 9 genera except *Zappa*) and amblyopine (*Odontamblyopus*, *Taenioides* and *Trypauchen*) gobies, which shows a deep divergence between the *Periophthalmus–Periophthalmodon* lineage and the other lineage containing all the other genera. Steppan et al. (2022) suggest that specialization to terrestriality evolved twice in the clade, but were unable to find support for the gradual, linear transition from aquatic to terrestrial mode of life within the clade. Similarly, Agorreta et al. (2013) proposed a clade consisting of eight oxudercine (*Apocryptes*, *Apocryptodon*, *Boleophthalmus*, *Oxuderces*, *Parapocryptes*, *Periophthalmus*, *Pseudapocryptes*, and *Scartelaos*) and three amblyopine (*Odontamblyopus*, *Taenioides* and *Trypauchen*) genera, which also shows an early divergence of *Periophthalmus* from the others. In neither of the phylograms by Steppan et al. (2022) or Agorreta et al. (2013), any correlation can be assumed between the development of terrestriality and shift in feeding habits from herbivory/omnivory to carnivory or specialized herbivory, as we proposed on the basis of Murdy's scheme. The three amblyopine genera described in the two studies are all carnivorous (Dôtu 1957; Rainboth 1996).

During the field work in the Mekong Delta, we have noticed that there is variability in the degree of amphibiousness among populations of the same oxudercine species. For example, we observed emersion of *O. nexipinnis* of short (usually less than 5 s) duration, which appears to be for feeding, from pools on a mudflat of Bac Lieu Province in the Mekong Delta (supplementary video S2), but we did not observe such behavior for the same species on a mudflat in the neighboring Soc Trang Province (Ishimatsu et al. unpublished). More data must be gained by field work on the feeding ecology of oxudercine gobies, together with more extensive analysis of their phylogenetic relationships, to better understand the possible relationship between feeding ecology and niche expansion to land in these fishes.

Supplementary Information The online version contains supplementary material available at https://doi.org/10.1007/s00435-022-00554-8.

Acknowledgements We would like to thank Ms. Mizuri Murata (Institute for East China Sea Research, Nagasaki University) and Dr. Hieu Van Mai (College of Aquaculture and Fisheries, Can Tho University) for their help during the field study; Dr. Nguyen Van Cong, the Dean of the College of Environment and Natural Resources, Can Tho University and Dr. Tran Dac Dinh, the College of Aquaculture and Fisheries, Can Tho University for arranging our trips to Mo O and providing preserved specimens for complementary observations; and a local fisherman for collecting samples.

Author contributions LXT contributed to the morphological analysis. LXT and AI contributed to writing the manuscript. All authors contributed to the final revision of the manuscript.

Funding This study was partly supported by Keidanren Nature Conservation Fund "Conservation and cleaning up of MoO mudflat, Mekong river-mouth".

Availability of data and materials The data that support the findings of this study are available from the corresponding author upon reasonable request.

Declarations

Conflict of interest The authors declare that they have no conflict of interest.

Ethical approval All experimental procedures were conducted with the permission of the Animal Care and Use Committee of the Institute for East China Sea Research, Nagasaki University, Japan (Permit Number #16-01).

References

Abidizadegan M, Saeid EP, Hosein R (2015) Partial morphometrics and meristic evaluation of the two species mudskippers: *Scartelaos tenuis* (Day, 1876) and *Periophthalmus waltoni* (Koumans, 1941) from the Persian Gulf, Bushehr, Iran. Int J Fish Aquat Stud 2:353–358

Agorreta A, Mauro DS, Schliewen U, Van Tassell JL, Kovačic M, Zardoya R, Rüber L (2013) Molecular phylogenetics of Gobioidei and phylogenetic placement of European gobies. Mol Phylogenet Evol 69:619–633. https://doi.org/10.1016/j.ympev.2013.07.017

Bucholtz RH, Meilvang AS, Cedhagen T, Christensen JT, Macintosh DJ (2009) Biological observations on the mudskipper *Pseudapocryptes elongatus* in the Mekong Delta, Vietnam. J World Aquac Soc 40:711–723. https://doi.org/10.1111/j.1749-7345.2009.00291.x

Chan KY (1989) The ecology of mudskippers (Pisces: Periophthalmidae) at the Mai Po Marshes Nature Reserve, Hong Kong. Master's thesis, Faculty of Science, University of Hong Kong

Chaudhuri A, Mukherjee S, Homechaudhuri S (2014) Food partitioning among carnivores within feeding guild structure of fishes inhabiting a mudflat ecosystem of Indian Sundarbans. Aquat Ecol 48:35–51. https://doi.org/10.1007/s10452-013-9464-x

Clayton DA (1993) Mudskippers. Oceanogr Mar Biol Annu Rev 31:507–577

Clayton D (2017) Feeding behavior: a review. In: Jaafar Z, Murdy EO (eds) Fishes out of water: biology and ecology of mudskippers. CRC Press, Boca Raton, pp 237–275

Dinh QM, Qin JG, Dittmann S, Tran DD (2014) Burrow morphology and utilization of the goby (*Parapocryptes serperaster*) in the Mekong Delta, Vietnam. Ichthyol Res 61:332–340. https://doi.org/10.1007/s10228-014-0402-2

Dinh QM, Qin JG, Dittmann S, Tran DD (2017) Seasonal variation of food and feeding in burrowing goby *Parapocryptes serperaster* (Gobiidae) at different body sizes. Ichthyol Res 64:179–189. https://doi.org/10.1007/s10228-016-0553-4

Dôtu Y (1957) On the bionomics and life history of the eel-like goby, *Odontamblyopus rubicundus* (Hamilton). Sci Bull Fac Agr Kyushu Univ 16:101–110

Fox J (2005) The R Commander: a basic statistic graphical user interface to R. J Stat Softw 14:1–42. https://doi.org/10.18637/jss.v014.i09

Fox J, Boutchet-Valat M (2020) Rcmdr: R Commander. R package version 2.7–1, https://socialsciences.mcmaster.ca/jfox/Misc/Rcmdr/

Ishimatsu A, Gonzales TT (2011) Mudskippers: front runners in the modern invasion of land. In: Patzner R, Van Tassell JL, Kovačić M, Kapoor BG (eds) The biology of gobies. Science Publishers, Enfield, pp 609–638

Ishimatsu A, Ishimatsu M (2021) An annotated translation of "Morphologie und Physiologie der Atmung bei wasser-, schlamm- und landlebenden Gobiiformes" by Elfriede Schöttle (1931). Bull Fac Fish Nagasaki Univ 101:1–149

Kassambara A, Mundt F (2020) Factoextra: Extract and visualize the results of multivariate data analyses. R Package Version 1.0.7. https://CRAN.R-project.org/package=factoextra

Khaironizam M, Norma-Rashid Y (2000) A new record of the mudskipper *Parapocryptes serperaster* (Oxudercinae: Gobiidae) from Peninsular Malaysia. Malay J Sci 19:101–104

Lê S, Josse J, Husson F (2008) FactoMineR: a package for multivariate analysis. J Stat Softw 25:1–18. https://doi.org/10.18637/jss.v025.i01

Liem KF (1974) Evolutionary strategies and morphological innovations: cichlid pharyngeal jaws. Syst Zool 22:425–441. https://doi.org/10.2307/2412950

Murdy EO (1989) A taxonomic revision and cladistic analysis of the oxudercine gobies (Gobiidae: Oxudercinae). Rec Aust Mus Suppl 11:1–93. https://doi.org/10.3853/j.0812-7387.11.1989.93

Murdy EO, Jaafar Z (2017) Taxonomy and systematics review. In: Jaafar Z, Murdy EO (eds) Fishes out of water: biology and ecology of mudskippers. CRC Press, Boca Raton, pp 1–36

Polgar G (2017) Emergent patterns in spatio-temporal ecology. In: Jaafar Z, Murdy EO (eds) Fishes out of water: biology and ecology of mudskippers. CRC Press, Boca Raton, pp 301–326

Rainboth WJ (1996) Fishes of the Cambodian Mekong: FAO species identification field guide for fishery purposes. FAO, Rome

Rathod SD, Patil NN (2009) Feeding habits of *Boleophthalmus dussumieri* (Cuv. & Val.) from Ulhas river estuary near Thane City, Maharashitra State. J Aqua Biol 24:153–159

Schöttle E (1931) Morphologie und Physiologie der Atmung bei wasser-, schlamm- und landlebenden Gobiiformes. Z Wiss Zool 140:1–114

Steppan SJ, Meyer AA, Barrow LN, Alhajeri BH, Al-Zaidan ASY, Gignac PM, Erickson GM (2022) Phylogenetics and the evolution of terrestriality in mudskippers (Gobiidae: Oxudercinae). Mol Phylogenet Evol 169:107416. https://doi.org/10.1016/j.ympev.2022.107416

Swennen C, Ruttanadakul N, Haver M, Piummongkol S, Prasertsongskum S, Intanai I, Chaipakdi W, Yeesin P, Horpet P, Detsathit S (1995) The five sympatric mudskippers (Teleostei: Gobioidea) of Pattani area, Southern Thailand. Nat Hist Bull Siam Soc 42:109–129

Takita T, Agusnimar, Ali AB (1999) Distribution and habitat requirements of oxudercine gobies (Gobiidae: Oxudercinae) along the Straits of Malacca. Ichthyol Res 46:131–138. https://doi.org/10.1007/BF02675431

Tran LX, Maekawa Y, Soyano K, Ishimatsu A (2020) Morphology of the feeding apparatus in the herbivorous mudskipper, *Boleophthalmus pectinirostris* (Linnaeus, 1758). Zoomorphology 139:231–243. https://doi.org/10.1007/s00435-020-00476-3

Tran LX, Maekawa Y, Soyano K, Ishimatsu A (2021) Morphological comparison of the feeding apparatus in herbivorous, omnivorous and carnivorous mudskippers (Gobiidae: Oxudercinae). Zoomorphology 140:387–404. https://doi.org/10.1007/s00435-021-00530-8

Westneat MW (2003) A biomechanical model for analysis of muscle force, power output and lower jaw motion in fishes. J Theor Biol 223:269–281. https://doi.org/10.1016/S0022-5193(03)00058-4

Yang KY, Lee SY, Williams GA (2003) Selective feeding by the mudskipper (*Boleophthalmus pectinirostris*) on the microalgal assemblage of a tropical mudflat. Mar Biol 143:245–256. https://doi.org/10.1007/s00227-003-1067-y